Comparison of dynamic models for a motorcycle during lowside fall

ANDREA BONCI, RICCARDO DE AMICIS, SAURO LONGHI AND EMANUELE LORENZONI
Università Politecnica delle Marche
Dipartimento di Ingegneria dell'Informazione
Via Brecce Bianche 12, 60131 Ancona
ITALY
{a.bonci, r.deamicis, sauro.longhi}@univpm.it, emanuele.lorenzoni@tin.it

Abstract: The controllers for active safety systems of motorcycles cannot be synthesized regardless by a suitable analytic dynamic model of the vehicle. Generally the analytical study and analysis of critical driving situations, falls and accidents is a complex task, since these events take place due to the simultaneity of different and complex phenomena. An analytical model able to capture the dynamics of a two-wheeled vehicle in curve is considered. In this paper the performance of the proposed model in describing the low side fall, a critical vehicle condition involving the safety of the rider, is investigated. The model has the minimum degree of complexity needed to describe complex dynamics and two different assumptions of accuracy have been made on it. The linearized version of the model has been compared with a nonlinearized version and the results have shown no substantial differences in the description of the lowside major dynamics.

Key–Words: Motorcycle dynamic, active safety systems, model-based control systems

1 Introduction

Nowadays, in the automobile industry, active safety systems have reached a high technological level and reliability. On the contrary, that has not happened for the powered two wheelers (PTW's), where the most used available system is the Anti-lock Braking System (ABS) [1]. According to recent statistics on motorcycles and mopeds fatalities [2], these kind of systems are desirable to increase rider safety. Currently, the control system design of safety devices for PTWs represents a challenging task.

Model-based design of control systems, widely used in automotive and aerospace sectors, represents an efficient and suitable approach to cope with this challenge [3]. Briefly, the model-based design approach for control systems requires the following steps: the modeling of the plant, the synthesis of the controller for the plant, its simulation and the controller deployment.

In such approach, the plant modeling is a core issue, mainly for systems having complex dynamic behaviours such as automobiles and motorcycles. In particular, the analysis of the motorcycle dynamics is even more complex. While the study of the automobile stability can be addressed adequately by considering the lateral and yaw degrees of freedom, for a motorcycle it is also required to add the roll and the steer angles.

When a motorcycle is leaned over in cornering, the longitudinal and lateral friction forces interact each other and this interaction increases with increased roll angle [4]. As a consequence of this feature, simple mathematical models are not suitable to describe high cornering accelerations during critical situations such as accidents and falls.

In literature [5], analytical models addressing the issues related to motorcycle's behaviour in curve usually makes some major assumptions such as: steady state cornering condition, the longitudinal and lateral contact forces acting on the tyres are linearized or do not interact each other [6]. In general, these works

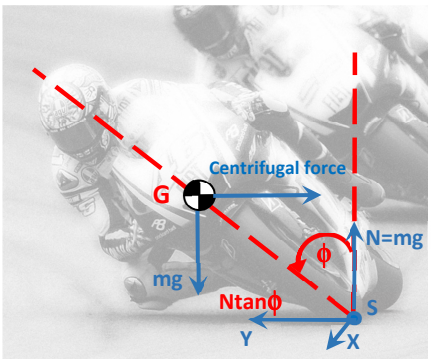

Figure 1: Motorcycle in cornering condition.

investigate on the effects related to the balancing of forces and moments during a turn as shown in Figure 1, where for a roll angle ϕ the relevant forces (frictional X, Y, centrifugal and gravitational mg) acting

on the vehicle system are reported. Their balancing yields the value of the lateral force Y needed to maintain in equilibrium the vehicle in curve that is equal to $N \tan \phi$, where N is the vertical load. However, falls and critical conditions cannot be captured under the aforementioned assumptions when strong acceleration or braking occur. As a result, a controller able to prevent falls should be synthesized by using more appropriate models. On the other hand, commercial multibody software allow to simulate adequately these complicated phenomena, but due to their black box nature they are not suitable for the purpose of synthesis of control systems.

Within the challenging task of investigating new safety devices preventing PTW's falls, and according to the model-based approach above mentioned, the present paper deals with its first step: the investigation of the behaviours of a proposed motorcycle analytical model during the lowside fall which is one of the most common motorcycle's fall. Here the motorcycle has been simulated in such typical dangerous condition that may potentially lead the driver to slide off the road and causing him serious injuries. In order to analyze the performance of the model in describing the fall, a comparison between a version of the model linearized with respect to the roll angle and the nonlinear version has been proposed.

The paper is organized as follows: the problem addressed in this paper is described in section 2. A description of the model is shortly summarized in section 3. In section 4 the lowside fall and the simulations results are presented. Section 5 completes the paper.

2 Problem statement and related works

The control of an active safety system for motorcycles cannot be synthesized regardless by a suitable dynamic model of the vehicle. The model should be able to describe its behaviour even during falls. Now, the following questions arise. Which analytical model may be suitable to describe the dynamics of the vehicle in complex situations such as the fall during cornering? What is the right trade-off between simulation accuracy and model's complexity? This article proposes the analysis of the results obtained by simulating a typical PTW's fall described with a motorcycle's analytic model. The model has the minimum degree of complexity needed to describe these dynamics (two rigid bodies) and two different assumptions of accuracy have been made on it: the roll angle's dynamic in both conditions linear and nonlinear have been considered. The comparison of the two behaviours shows the effects of the roll angle's dynamic on the accuracy of the results of the model during fall situations where huge roll angles are involved.

An analytical model is used to address the lowside phenomenon whose complex dynamics usually requires the use of multibody software. The model is based on the author's prior works. It removes the condition of steady-state in cornering and introduces the rear traction given by the engine, the tyre friction forces and their interaction. The proposed model has been already tested in several situations: in [7] the motorcycle dynamics in straight running, acceleration and braking with slippages have been considered; furthermore, the cornering situation with no slippages has been analyzed; in [8] the author's model has been compared with a well established model proposed in literature considering the motorcycle in cornering condition with no slippages; in [9] the same model has been compared with its nonlinear version with respect the lean angle, here the pure rolling during the cornering has been assumed for both the wheels. In this paper a further analysis of the model in cornering condition with slippages has been done.

Generally the analytical study and analysis of critical driving situations, falls and accidents, is a complex task since these events take place due to the simultaneity of different circumstances involving the trim of the motorcycle in motion, the speed and the increase of lean angle. This analytical complexity augments when considering the loss of adherence both in acceleration and braking that may lead the panicked rider to the typical lowside fall. A lowside may occur while approaching a curve with excessive velocity and braking. Due to the wheels loss of adherence, the rider loses the vehicle control and they both fall laterally. Lowside critical aspects are described in the section 4. In the next section the equations of motion of the model are briefly summarized.

3 Summary of the analytic model

As shown in Figure 2, the model consists of two rigid bodies, the rear frame with mass centre G_r which includes the rider, the engine and the rear wheel with radius R_r, and the front frame with mass centre G_f which includes the steering mechanism and the front wheel with radius R_f. Besides, the geometric parameters h, j, l and b represent the heights of the two rigid bodies respect to the ground level and the distances of the wheels from the point A respectively. The model has 7 degrees of freedom (dofs): the longitudinal and lateral velocity of the motorcycle respectively $\dot{x}_1$, $\dot{y}_1$, the yaw angle ψ, the roll angle ϕ, the rotation around the steer δ and the tyre rotations $\dot{\theta}_r$ and $\dot{\theta}_f$. The vertical dynamic does not provide a fundamental contri-

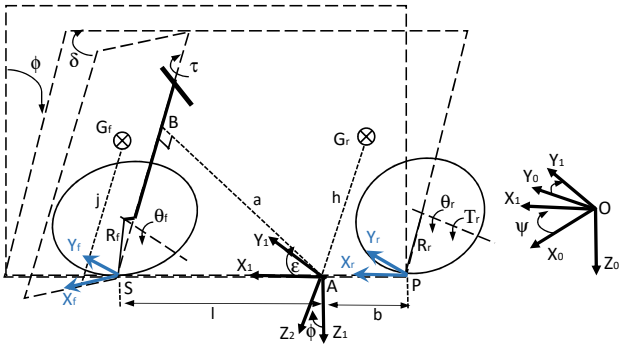

Figure 2: Geometric parameters of the model.

bution to the lowside fall dynamic hence it can be neglected by the model. Figure 2 also shows the reference frames needed to describe the position and orientation of the two rigid bodies G_r and G_f as reported in table 1. In order to simulate the motion of the vehicle in acceleration and braking, the model takes into account the traction T_r provided by the rear engine. The rider is rigidly attached to the rear body and he maneuvers the motorcycle by applying the torque τ on the handlebar. Finally, X_f, Y_f, X_r and Y_r are the longitudinal and lateral friction forces applied at the front and rear tyre on the road contact points S and P respectively.

reference frame (r.f.)	description
$\Sigma_0(O, X_0, Y_0, Z_0)$	inertial reference frame
$\Sigma_1(A, X_1, Y_1, Z_1)$	rear reference frame rotating Σ_0 of a yaw angle ψ wrt Z_0
$\Sigma_2(A, X_2, Y_2, Z_2)$	rear reference frame rotating Σ_1 of a roll angle ϕ wrt X_1
$\Sigma_3(A, X_3, Y_3, Z_3)$	rear reference frame rotating Σ_2 of a pitch angle ϵ wrt Y_2
$\Sigma_4(B, X_4, Y_4, Z_4)$	front reference frame rotating Σ_3 of a steer angle δ wrt Z_3

Table 1: The reference frames.

3.1 Equations of motion

After defining the geometry and the model reference frames, the equations of motion have been derived using the Lagrangian equation:

$$\frac{d}{dt}\left(\frac{\partial T}{\partial \dot{q}}\right) - \frac{\partial T}{\partial q} + \frac{\partial V}{\partial q} = Q_q, \qquad (1)$$

where:

- T is the kinetic energy;
- V is the potential energy;
- $q = [\dot{x}_1\ \dot{y}_1\ \dot{\psi}\ \dot{\phi}\ \dot{\delta}\ \dot{\theta}_r\ \dot{\theta}_f]^T$ is the system's dofs vector;
- Q_q is the vector of the generalized external forces that are functions of the friction forces (Figure 2).

Sobstituting the kinetic energy T and the potential energy V derived in [9], 7 nonlinear second order differential equations are obtained. In order to reduce their complexity, in [7] and [8] these equations have been linearized around the vertical position considering $(\phi, \delta) = (0, 0)$.

For a motorcycle on a curve the steer angle δ remains limited to a few degrees endorsing the linearization assumption, while the lean angle ϕ usually can assume large values. Therefore, the small approximation for the roll angle may be excessive. In order to investigate the accuracy of the linearized model in describing a lowside fall in cornering, it has been compared with the same model with no roll angle linearization assumption. This model has been derived in [9]. For the sake of semplicity all the equations of motion with no roll linearization are reported in Appendix A.

3.2 The contact forces

In order to describe the motorcycle behaviours on a curve and in critical situations the tyre friction forces have to be modeled adequately. Indeed, they transfer the power provided by the motor through the tyre-ground contact and they are needed to push the vehicle and keep it in balance while running the trajectory in curve.

The literature proposes several tyre models, among which, purely theoretical models such as the brush model can be found [10]. This model is able to describe most of the tyre conditions. Other kinds of models are empirical hence they do not provide any theoretic foundamentals but deliver accurate descriptions of the tyres behaviour. Among the empirical models, the "magic formula" became the standard for the vehicle dynamic simulations [11]. The model

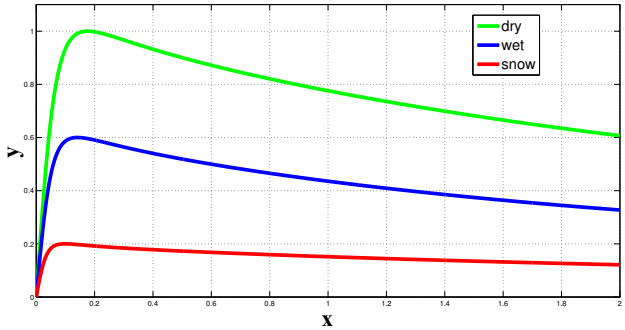

Figure 3: The magic formula for different road conditions.

is described by the following expression:

$$y(x) = D\sin[C\arctan\{Bx - E(Bx - \arctan(Bx))]\}, \quad (2)$$

where the variables and parameters in the equation are: x is the input variable, y is the output variable, B is the stiffness factor, C is the form factor, D is the peak value of the curve and E is the bending factor. By varying the values of parameters B, C, D and E it is possible to consider the friction forces for different road conditions, as shown in Figure 3. The peak value D represents the maximum value of the force generated by the tyre and depends on the coefficient of friction μ and the vertical load F_z acting on the wheel:

$$D = \mu F_z. \quad (3)$$

The equation 2 allows to calculate:

- the longitudinal forces X_r and X_f as a function of the longitudinal slip;
- the lateral forces Y_r and Y_f as a function of the lateral slip angle.

Based on the SAE J670 definitions, the longitudinal slip λ is defined as:

$$\lambda = -\frac{\dot{x} - R\dot{\theta}}{\dot{x}}, \quad (4)$$

where $\dot{x}$, $\dot{\theta}$ and R are respectively the forward velocity of the vehicle, the wheel angular velocity and the wheel's radius. The coefficient λ is positive in traction and negative in braking. The lateral slip α is defined as:

$$\tan\alpha = -\frac{\dot{y}}{\dot{x}}, \quad (5)$$

where $\dot{x}$ and $\dot{y}$ are the forward and lateral velocity of the wheel. Using expressions (4) and (5), the magic formula (2) for the longitudinal and lateral force hold:

$$F_{x0}(\lambda, F_z) = F_z\, D_x \sin[C_x \arctan\{B_x\lambda - E(B_x\lambda - \arctan(B_x\lambda))]\}, \quad (6)$$

$$F_{y0}(\alpha, F_z) = F_z\, D_y \sin[C_x \arctan\{B_x\alpha - E(B_x\alpha - \arctan(B_x\alpha))]\}, \quad (7)$$

where λ and α are given respectively by (4) and (5). For motorcycle tyres, the roll angle (or camber angle) can reach up to $50°$-$55°$ in extremis cases. In order to take into account the lateral slip and the camber angle, it is possible to define the equivalent sideslip as:

$$\alpha_{eq} = \alpha + \frac{k_\phi}{k_\alpha}\phi, \quad (8)$$

where α is the lateral slip defined in (5), ϕ is the wheel camber angle, k_ϕ and k_α are respectively the camber and the cornering stiffnesses. Replacing α with α_{eq}, the lateral force (7) becomes:

$$F_{y0}(\alpha_{eq}, F_z) = F_z\, D_y \sin[C_x \arctan\{B_x\alpha_{eq} - E(B_x\alpha_{eq} - \arctan(B_x\alpha_{eq}))]\}. \quad (9)$$

Besides, by considering the interaction between the longitudinal and lateral forces, the theoretical slips σ_x and σ_y can be defined as follows:

$$\begin{cases} \sigma_x = \dfrac{\lambda}{1+\lambda} \\ \sigma_y = \dfrac{\tan\alpha_{eq}}{1+\lambda}. \end{cases} \quad (10)$$

By introducing the slip magnitude σ:

$$\sigma = \sqrt{\sigma_x^2 + \sigma_y^2}. \quad (11)$$

the friction forces are:

$$\begin{cases} X' = \dfrac{\sigma_x}{\sigma} F_{x0} \\ Y' = \dfrac{\sigma_y}{\sigma} F_{y0}. \end{cases} \quad (12)$$

To take into account the time delay of the tyres the following equations must be introduced:

$$\begin{cases} \dfrac{\xi_x}{\dot{x}_1}\dot{X} + X = X' \\ \dfrac{\xi_y}{\dot{x}_1}\dot{Y} + Y = Y', \end{cases} \quad (13)$$

where ξ_x and ξ_y are the tyre longitudinal and lateral relaxation lengths and X' and Y' are given by (12). The expressions of X and Y computed in (13) for the rear and front tyre are the friction forces of the model.

3.3 Slippages and front wheel camber angle

To calculate the theoretical slips given in (10) the input quantities ϕ, λ and α must be computed for both the wheels. Referring to Figure 2 and by using equation (4), the rear and front longitudinal slip λ_r and λ_f are simply:

$$\lambda_r = -\frac{\dot{x}_1 + R_r\dot{\theta}_r - R_r\sin\phi\dot{\psi}}{\dot{x}_1}. \quad (14)$$

$$\lambda_f = -\frac{\dot{x}_1 + R_f\dot{\theta}_f\cos\delta\cos\epsilon}{\dot{x}_1}, \quad (15)$$

Equations (14) and (15) show that the two longitudinal slips are related to the motorcycle longitudinal velocity $\dot{x_1}$, the rear and the front angular velocities $\dot{\theta}_r$,

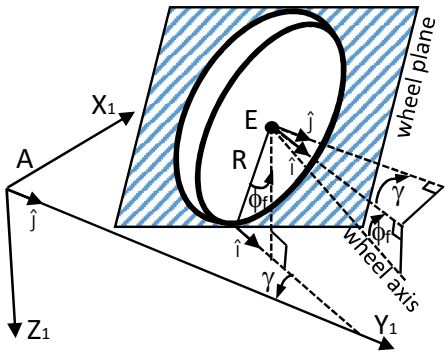

Figure 4: The front camber angle.

$\dot{\theta}_f$ and the dofs ϕ, $\dot{\psi}$ and δ. The longitudinal slips are therefore being affected by most of the variables of the model. Figure 4 shows the front wheel in some generally displaced position and the front camber angle ϕ_f can be easily computed as:

$$\sin\phi_f = \sin\phi + \delta\cos\phi\sin\epsilon, \tag{16}$$

while for the rear wheel the camber angle ϕ_r is simply:

$$\phi_r = \phi. \tag{17}$$

Referring to Figure 2 and using equation (5), the rear and the front sideslip angle α_r and α_f are:

$$\alpha_r = \frac{b\dot{\psi} - \dot{y}_1}{\dot{x}_1}. \tag{18}$$

$$\alpha_f = \delta\cos\epsilon - \frac{\dot{y}_1 + l\dot{\psi} - t\dot{\delta}}{\dot{x}_1}, \tag{19}$$

where l and t are the parameters listed in table 2 reported in Appendix A.

4 Lowside fall simulations

A motorcycle may experience a lowside fall while entering in a curve with excessive speed and instinctively the rider brakes hard to keep the trajectory. The strong rear braking results in the rear wheel losing lateral adherence and the increase of the roll and yaw angles. In case the panicking rider ignores the loss of adherence and keeps on braking, the slippage never stops because the lateral force acting on the rear wheel is always lesser than the force necessary to keep the vehicle in balance. In particular, the required friction force is proportional to $\tan\phi$ (Figure 1). In this case the roll angle increases progressively and the vehicle ends up to fall laterally and drag the rider down (Figure 5).

Figure 5: The lowside fall. (Source: www.zimbio.com)

In the following it will be investigated the effect of the roll angle on the motorcycle dynamic by simulating the vehicle during a lowside fall and comparing the behaviour of the linearized model against the nonlinear model. In the following figures the trends of the

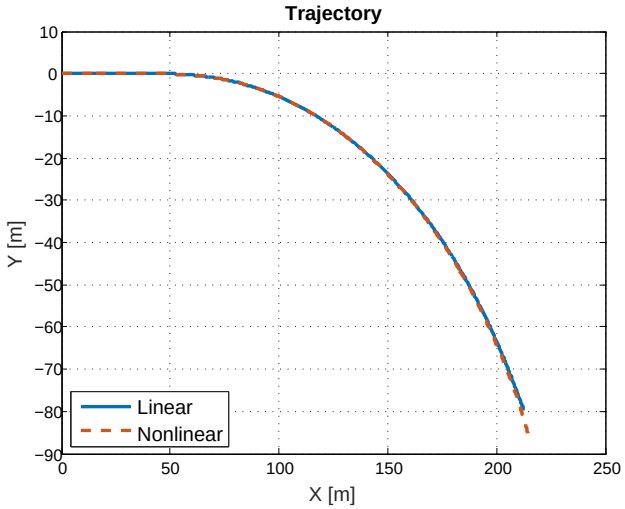

Figure 6: The curve.

variables involved in the simulations are compared. The subscripts "L" and "NL" stand for the linear and the nonlinear case respectively, "r" and "f" stand for rear and front. The trajectory, the roll angle ϕ, the yaw angle ψ, the lateral forces Y_r and the longitudinal forces X_r acting on the rear wheel, the rear wheel's angular velocity $\dot{\theta}_r$, the front wheel's angular velocity $\dot{\theta}_f$ have been compared. The simulations start with the motorcycle runnnig the trajectory depicted in Figure 6. The vehicle engages the curve at 40 m/s (144 km/h) with roll angle ϕ of about 40°, as shown in Figure 8. The trends of the variables yield by the linear model and the nonlinear model are very similar till the brake is applied. Figure 7 shows the strong negative rear torque applied on the rear wheel in the time window 5-6.5 seconds. This torque simulates the hard

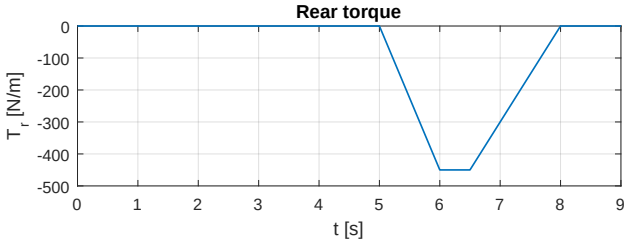

Figure 7: The rear torque.

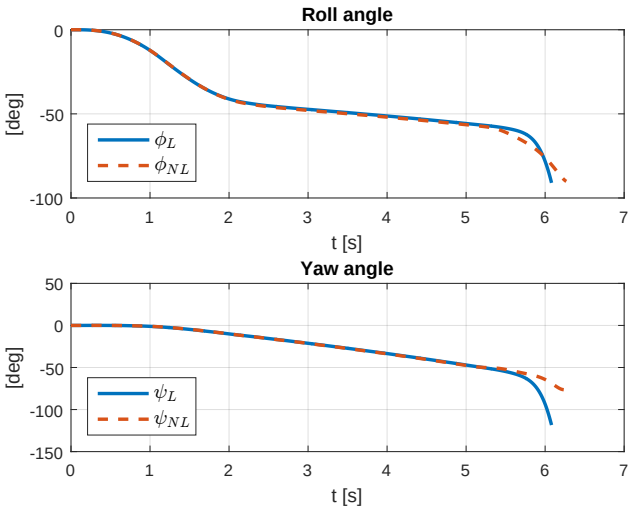

Figure 8: The roll and yaw angles.

braking applied by the rider. As shown in Figure 9,

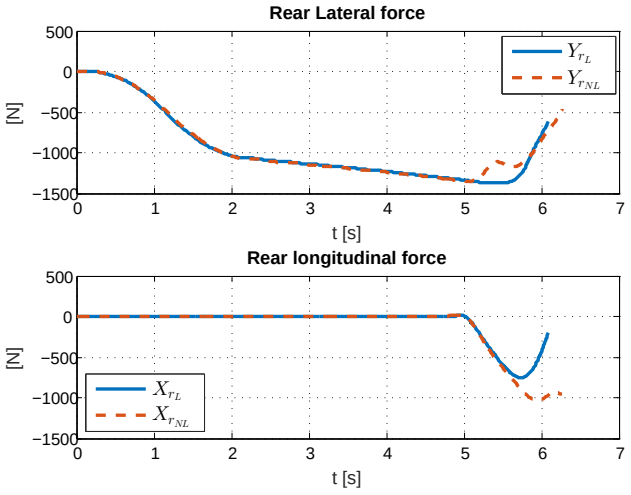

Figure 9: The rear lateral and longitudinal forces.

during the same time window the longitudinal forces X_{r_L}, $X_{r_{NL}}$ acting on the rear wheel (also known as the braking forces) show a fast growing trend as expected. Figure 10 shows that the braking action leads to an increase in the rear longitudinal slip angles σ_{x_L},

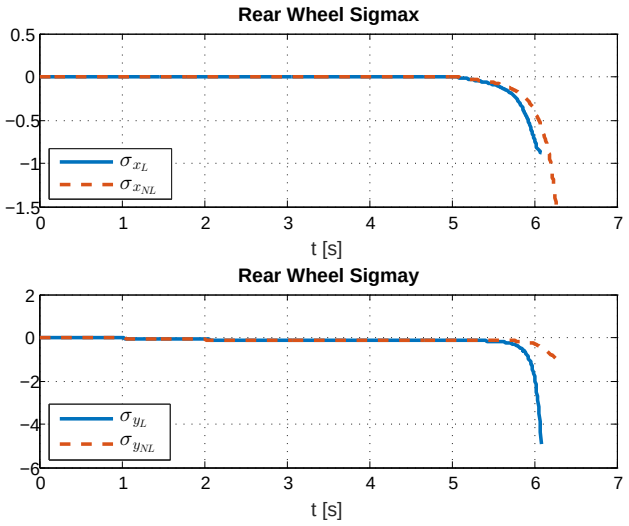

Figure 10: The rear theoretical slips.

$\sigma_{x_{NL}}$. As a result of the longitudinal slip, the rear lateral slips σ_{y_L}, $\sigma_{y_{NL}}$ increase as well because the rear lateral force Y_r needed to maintain the vehicle in balance are reached with a greater rear slip angle in both linear and nonlinear cases. The rear wheel's angular velocities $\dot{\theta}_{r_L}$, $\dot{\theta}_{r_{NL}}$ decrease more strongly with respect to the relevant front wheel's angular velocities $\dot{\theta}_{f_L}$, $\dot{\theta}_{f_{NL}}$ (Figure 11). As the braking force

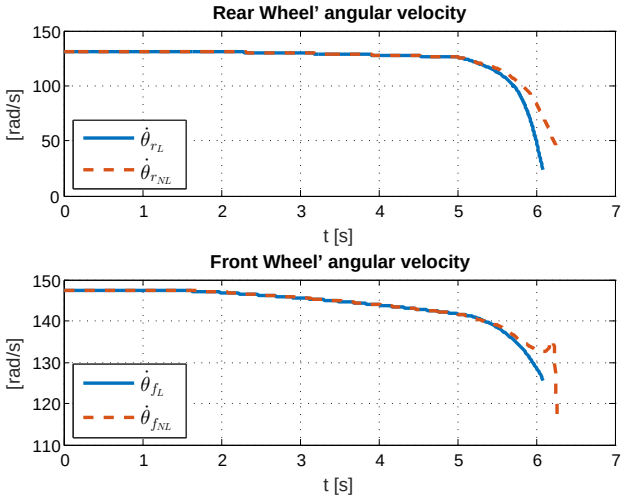

Figure 11: The rear and front angular velocities.

reaches its maximum at 6 seconds (Figure 7), a slight difference on the rear wheel's angular velocities can be observed between the linear and nonlinear cases, but still they maintain the same trend. The roll angles drop progressively in both cases although the trends are slightly different as shown in Figure 8. In Figure 9 the lateral forces Y_{r_L} and $Y_{r_{NL}}$ acting on the rear wheel are shown. During the braking, the force

Y_{r_L} starts decreasing more rapidly than $Y_{r_{NL}}$ but in both cases these values tend to decrease progressively and they are not sufficient to keep the motorcycle in balance hence the slip angle of the rear wheel continues to grow as well as the roll angles ϕ_L and ϕ_{NL}. At 6.5 seconds the rider starts decelerating but the roll angle has now reached such a value that it is impossible for the rider to regain the correct attitude of the vehicle in both cases. Indeed, around 6.2 seconds the motorcycle reaches 90° in the roll angle hence it falls down and the simulation ends. The trajectories depicted in

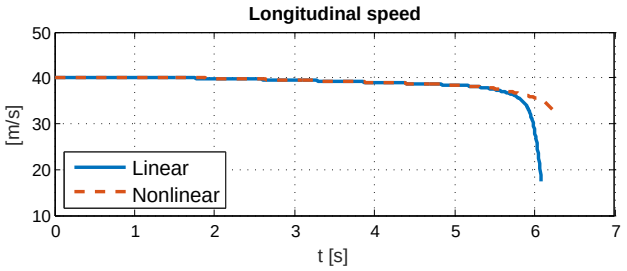

Figure 12: The longitudinal velocity.

Figure 6 show little difference between the linear and the nonlinear case, precisely in the first case the fall occurs slightly sooner than in the nonlinear case. The graphs clearly show that the linearization on the roll angle ϕ is able to describe most of a lowside fall dynamic, in particular this event occurs slightly in advance respect to the nonlinear case, but the trajectory run by the vehicles are very similar. The major difference stands on the final longitudinal velocity that in the linear case reaches a smaller value (Figure 12). It is worth noting that the general vehicle dynamic in this critical condition is strongly affected by the tyres friction forces. The trends of the dynamics variables obtained in the simulations are in line with what was expected. This results push the authors to address a deeper analysis of the model in future works.

5 Conclusion

In this paper the authors have investigated furtherly the performance of a motorcycle's analytical model in describing the low side fall, a critical driving condition that may put at risk the safety of the driver. Authors proposes this model as a resource for designing model-based safety control systems for PTWs. The rear traction, an adequate modelling of longitudinal and lateral dynamic, tyre friction forces and their interactions they are all considered by the model and make it suitable to capture most of the complex motorcycle dynamics arising in cornering, where the vehicle may experience extreme loss of adherence due to excessive acceleration or braking. In order to better evaluate the effects of the roll dynamic on the accuracy of the lowside simulation a linear version and a nonlinear version of the same model have been compared. The results show that in spite of the large roll angles involved in the low side phenomena, the linear version is able to capture such critical condition. This result confirms the high influence of the tyre forces on the general vehicle dynamic. Given the rapid evolution of the fall in this specific case, the linear simulation represents an encouraging approximation of the nonlinear phenomenon and it deserves further analysis that will be presented in the next works along with others studies on similar critical conditions.

Appendix A

The complete set of equations of motion:

$$[\ddot{x}_1] \quad (M_f + M_r)(\ddot{x}_1 - \dot{y}_1\dot{\psi}) - (M_r h - M_f j)\sin\phi\ddot{\psi} - M_f k\dot{\psi}^2 - 2(M_r h + M_f j)\cos\phi\dot{\phi}\dot{\psi} - 2M_f e\cos\phi\dot{\psi}\dot{\delta} - M_f e\cos\epsilon\dot{\delta}^2 = X_r + X_f \tag{20}$$

$$[\ddot{\theta}_r] \quad (i_{ry} + i\lambda^2)\ddot{\theta}_r + (i_{ry} + i\lambda)\sin\phi\ddot{\psi} + (i_{ry} + i\lambda)\cos\phi\dot{\phi}\dot{\psi} = R_r X_r + T_r \tag{21}$$

$$[\ddot{\theta}_f] \quad i_{fy}\ddot{\theta}_f + i_{fy}\sin\phi\ddot{\psi} - i_{fy}\cos\epsilon\dot{\phi}\dot{\delta} + i_{fy}\cos\phi\dot{\psi}\dot{\phi} + i_{fy}\sin\epsilon\cos\phi\dot{\psi}\dot{\delta} = R_f X_f \tag{22}$$

$$[\ddot{y}_1] \quad (M_f + M_r)(\ddot{y}_1 + \dot{x}_1\dot{\psi}) + (M_r h + M_f j)\cos\phi\ddot{\phi} + M_f e\cos\phi\ddot{\delta} + M_f k\ddot{\psi} - (M_r h + M_f j)\sin\phi\dot{\psi}^2 - (M_r h + M_f j)\sin\phi\dot{\phi}^2 - M_f\dot{\delta}^2 e\sin\epsilon\sin\phi - 2M_f\dot{\delta}\dot{\phi}e\sin\phi = Y_r + Y_f \tag{23}$$

$$[\ddot{\psi}] \quad -(M_r h - M_f j)\sin\phi\ddot{x}_1 + M_f k\ddot{y}_1 + (I_{rz}\cos\phi^2 + I_{fy}\sin\phi^2 + I_{ry}\sin\phi^2 + I_{fz}\cos\epsilon^2\cos\phi^2 + I_{fx}\cos\phi^2\sin\epsilon^2 + M_f k^2 + (M_r h^2 + M_f j^2)\sin\phi^2)\ddot{\psi} + (M_f jk + I_{fz}\cos\epsilon\sin\epsilon - I_{fx}\cos\epsilon\sin\epsilon - C_{rxz})\cos\phi\ddot{\phi} + (M_f ek + I_{fz}\cos\epsilon)\cos\phi\ddot{\delta} + (I_{ry} + I\lambda)\sin\phi\ddot{\theta}_r + I_{fy}\sin\phi\ddot{\theta}_f + (I_{ry} + I\lambda)\cos\phi\dot{\phi}\dot{\theta}_r + I_{fy}\cos\phi\dot{\phi}\dot{\theta}_f + I_{fy}\sin\epsilon\cos\phi\dot{\delta}\dot{\theta}_f + (M_r h + M_f j)\sin\phi\dot{y}_1\dot{\psi} + M_f k\dot{x}_1\dot{\psi} + (C_{rxz} + I_{fx}\cos\epsilon\sin\epsilon - I_{fz}\cos\epsilon\sin\epsilon - M_f jk)\dot{\phi}^2 + 2(M_r h^2 + M_f j^2 - I_{fz}\cos\epsilon^2 - I_{fx}\sin\epsilon^2 + I_{fy} + I_{ry} - I_{rz})\sin\phi\cos\phi\dot{\phi}\dot{\psi} + 2(I_{fy}\sin\epsilon - I_{fx}\sin\epsilon + M_f ej)\sin\phi\cos\phi\dot{\psi}\dot{\delta} + (I_{fx}\cos\epsilon - I_{fy}\cos\epsilon - I_{fz}\cos\epsilon - 2M_f ek)\sin\phi\dot{\phi}\dot{\delta} + M_f ef\sin\phi\dot{\delta}^2 = Y_f l - Y_r b \tag{24}$$

$$[\ddot{\phi}] \quad (M_r h + M_f j)\cos\phi\ddot{y}_1 + (I_{fz}\cos\epsilon\sin\epsilon - I_{fx}\cos\epsilon\sin\epsilon - C_{rxz} + M_f jk)\cos\phi\ddot{\psi} + (I_{fz} +$$

$$I_{rx} + M_f a^2 + M_f e^2 + M_r h^2 + I_{fx}\cos\epsilon^2 - I_{fz}\cos\epsilon^2 + 2M_f ae - M_f a^2\cos\epsilon^2 - M_f e^2\cos\epsilon^2 + M_f f^2\cos\epsilon^2 - 2M_f ae\cos\epsilon^2 + 2M_f af\cos\epsilon\sin\epsilon + 2M_f ef\cos\epsilon\sin\epsilon)\ddot{\phi} + (I_{fz}\sin\epsilon + M_f ej)\ddot{\delta} - (I_{ry} + i\lambda)\cos\phi\dot{\theta}_r\dot{\psi} - I_{fy}\cos\phi\dot{\psi}\dot{\theta}_f - I_{fy}\cos\epsilon\dot{\delta}\dot{\theta}_f + (M_r h + M_f j)\cos\phi\dot{x}_1\dot{\psi} + (I_{fx} - I_{fy} + I_{fz})\cos\epsilon\sin\phi\dot{\psi}\dot{\delta} + (I_{fx} - I_{fy} - I_{ry} + I_{rz} - M_f a^2 - M_f e^2 - 2M_f ae - M_r h^2 - I_{fx}\cos\epsilon^2 + I_{fz}\cos\epsilon^2 + M_f a^2\cos\epsilon^2 + M_f e^2\cos\epsilon^2 - M_f f^2\cos\epsilon^2 + 2M_f ae\cos\epsilon^2 - 2M_f af\cos\epsilon\sin\epsilon - 2M_f ef\cos\epsilon\sin\epsilon)\sin\phi\cos\phi\dot{\psi}^2 + Z_f t\delta\cos\phi - M_r gh\sin\phi - Y_f t\delta\sin\phi - M_f eg\cos\phi\sin\delta - M_f fg\cos\epsilon\sin\phi - M_f ag\sin\epsilon\sin\phi - M_f eg\cos\delta\sin\epsilon\sin\phi = 0 \quad (25)$$

$$[\ddot{\delta}] \quad M_f e\cos\phi\ddot{y}_1 + (I_{fz}\cos\epsilon + M_f ek)\cos\phi\ddot{\psi} + (I_{fz}\sin\epsilon + M_f ej)\ddot{\phi} + (M_f e^2 + I_{fz})\ddot{\delta} + M_f e\cos\phi\dot{x}_1\dot{\psi} + I_{fy}\cos\epsilon\dot{\phi}\dot{\theta}_f - I_{fy}\cos\phi\sin\epsilon\dot{\psi}\dot{\theta}_f + (I_{fy} - I_{fx} - I_{fz})\cos\epsilon\sin\phi\dot{\phi}\dot{\psi} + (I_{fx}\sin\epsilon - I_{fy}\sin\epsilon - M_f ej)\sin\phi\cos\phi\dot{\psi}^2 + K\dot{\delta} + Y_f t\cos\phi + Z_f t\sin\phi - X_f t\delta\cos\epsilon - M_f eg\sin\phi + Z_f t\delta\cos\phi\sin\epsilon - Y_f t\delta\sin\epsilon\sin\phi - M_f eg\delta\cos\phi\sin\epsilon = \tau. \quad (26)$$

The motorcycle physical parameters are listed in table 2.

parameter	notation	value	u.m. (SI)
M_f	mass of front frame	30.6472	kg
M_r	mass of rear frame	217.4492	kg
Z_f	front vertical force	-1005.3	N
I_{rx}	rear frame inertia x axis	31.184	kg m^2
I_{rz}	rear frame inertia z axis	21.069	kg m^2
C_{rxz}	product of inertia xz	1.7354	kg m^2
I_{fx}	front frame inertia x axis	1.2338	kg m^2
I_{fz}	front frame inertia z axis	0.442	kg m^2
$i_{fy} = i_{ry}$	front and rear wheel inertias	0.7186	kg m^2
ϵ	caster angle	0.4715	rad
a	distance between A and B	0.9485	m
b	distance between A and P	0.4798	m
e	x position of G_r	0.024384	m
f	z position of G_f	0.028347	m
h	z position of G_r	0.6157	m
l	distance between A and S	0.9346	m
R_r	rear wheel radius	0.3048	m
R_f	front wheel radius	0.3048	m
t	trail	0.11582	m

Table 2: Motorcycle physical parameters.

References:

[1] P. Seiniger, K. Schröter, J. Gail, Perspectives for motorcycle stability control systems, *Accident Analysis & Prevention*, Volume 44, Issue 1, 2012, pp. 74-81.

[2] European Road Safety Observatory, `https://ec.europa.eu/transport/road_safety/specialist/erso_en`

[3] J. Reedy, S. Lunzman, Model Based Design Accelerates the Development of Mechanical Locomotive Controls, *SAE Technical Paper*, 2010.

[4] C. Koenen, The dynamic behaviour of a motorcycle when running straight ahead and when cornering, *PhD Dissertation*, 1983, TU Delft.

[5] V. Cossalter, A. Doria, R. Lot, Steady Turning Of Two Wheel Vehicles, *Vehicle System Dynamics*, 31, 3, 1999, pp. 157-181.

[6] R. Lot, A Motorcycle Tires Model for Dynamic Simulations: Theoretical and Experimental Aspects, *Meccanica*, vol. 39, 2004, pp. 207-220.

[7] A. Bonci, R. De Amicis, S. Longhi, G. A. Scala and A. Andreucci, Motorcycle lateral and longitudinal dynamic modeling in presence of tyre slip and rear traction, *21st International Conference on Methods and Models in Automation and Robotics (MMAR)*, Miedzyzdroje, 2016, pp. 391-396.

[8] A. Bonci, R. De Amicis, S. Longhi, E. Lorenzoni and G. A. Scala, A motorcycle enhanced model for active safety devices in intelligent transport systems, *12th IEEE/ASME International Conference on Mechatronic and Embedded Systems and Applications (MESA)*, Auckland, 2016, pp. 1-6.

[9] A. Bonci, R. De Amicis, S. Longhi, E. Lorenzoni and G. A. Scala, Motorcycle's lateral stability issues: Comparison of methods for dynamic modelling of roll angle, *20th International Conference on System Theory, Control and Computing (ICSTCC)*, Sinaia, 2016, pp. 607–612.

[10] H. Dugoff, P. Fancher, L. Segel, Tire performance characteristics affecting vehicle response to steering and braking control inputs. *Ed. by Michigan Highway Safety Research Institute*, 1969.

[11] A. T. van Zanten, Bosch ESP Systems: 5 Years of Experience, *SAE Technical Paper*, 2000.